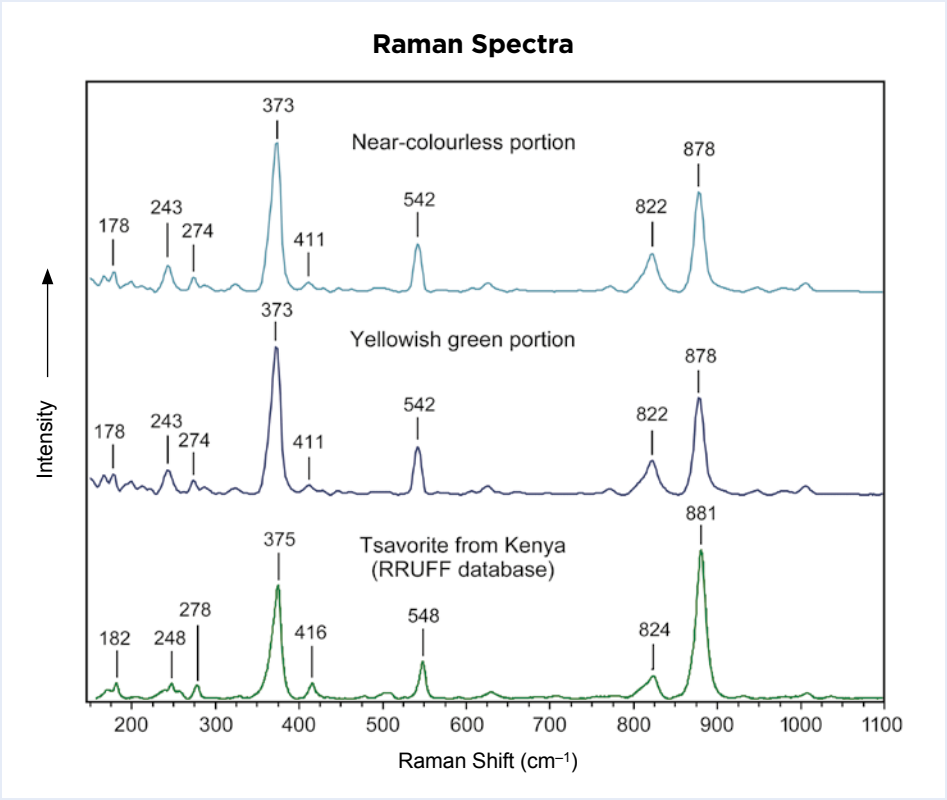

Figure 9: Representative background-corrected Raman spectra of the nearly colourless and yellowish green zones of the bicoloured grossular from Tanzania are compared to typical tsavorite from Kenya.

References

Feneyrol, J., Giuliani, G., Ohnenstetter, D., Rondeau, B., Fritsch, E., Fallick, A.E., Ichang'i, D., Omito, E. *et al.* 2014. New typology and origin of tsavorite based on trace-element chemistry. *European Journal of Mineralogy*, **26**, 293–308, https://doi.org/10.1127/0935-1221/2014/0026-2367.

Kane, R.E., Kampf, A.R. & Krupp, H. 1990. Well-formed tsavorite gem crystals from Tanzania. *Gems & Gemology*, **26**(2), 142–148, https://doi.org/10.5741/gems.26.2.142.

Kolesov, B.A. & Geiger, C.A. 1998. Raman spectra of silicate garnets. *Physics and Chemistry of Minerals*, **25**(2), 142–151, https://doi.org/10.1007/s002690050097.

Zwaan, J.C. 2014. Gem Notes: Bicoloured grossular from Kambanga, Kenya. *Journal of Gemmology*, **34**(3), 195–197.

Pargasite from Lajuar Madan, Badakhshan, Afghanistan

During the February 2018 gem shows in Tucson, Arizona, USA, gem dealer Dudley Blauwet (Dudley Blauwet Gems, Louisville, Colorado, USA) loaned the authors two faceted samples of pargasite from Afghanistan for gemmological examination. The specimens were cut from rough material that was obtained by Blauwet in June 2014, and was reportedly mined from the famous skarn-hosted lapis lazuli deposits near Lajuar Madan in the Kuran wa Munjan District of Badakhshan Province.

The two stones consisted of transparent faceted oval cuts weighing 0.27 ct (5.22 × 3.54 × 2.33 mm) and 0.65 ct (6.68 × 4.98 × 3.22 mm), and were light yellowish brown (Figure 10). The RIs of both stones were 1.620–1.642,

Figure 10: These yellowish brown gems (left, 0.65 ct; right, 0.27 ct) from Badakhshan, Afghanistan, proved to be pargasite. Photo by J. C. Zwaan.

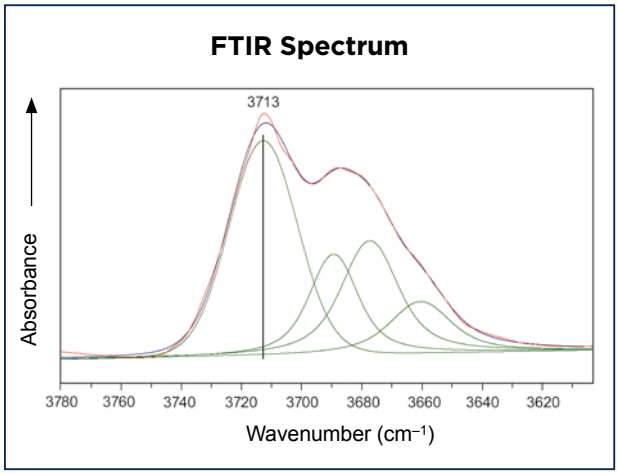

Figure 11: A representative FTIR spectrum in the OH-stretching region corresponds to the spectrum of pargasite (cf. Day *et al.* 2018). The red curve is the spectrum of the 0.27 ct sample and the dark blue curve is the resultant fitted line from the deconvolution of the spectrum (as shown by the green traces).

yielding a birefringence (DR) of 0.022. The optic character was biaxial positive. Average hydrostatic SG values were 3.10 and 3.07, respectively. Using a calcite dichroscope, weak pleochroism in pale yellow and slightly brownish yellow colours was discerned. The gems fluoresced very weak red under long-wave UV radiation, and moderate yellow (0.27 ct) or weak yellow (0.65 ct) under short-wave UV.

The 0.27 ct oval contained parallel growth tubes and a cluster of small mineral inclusions near the pavilion. Raman analysis identified diopside, zircon and sodalite in the cluster. The 0.65 ct oval contained partially healed fissures consisting of rectangular multiphase inclusions. Due to their small sizes and positions, these inclusions could not be analysed in further detail.

Using standard gemmological testing alone, it was difficult to identify these stones with confidence. From the optical data, the samples were established as amphiboles, and their optic character prevents confusion with tourmaline. However, the RI, birefringence and SG values closely match those of various amphiboles, including richterite (RI 1.605–1.641, DR 0.017–0.022, SG 2.97–3.45), pargasite (RI 1.613–1.650, DR 0.020–0.022, SG 3.07–3.81) and edenite (RI 1.606–1.672, DR 0.023–0.025, SG 3.00–3.06; Dedeyne & Quintens 2007). The SG values are at the highest and lowest limits for edenite and pargasite, respectively.

Day *et al.* (2018) characterised colourless gem-quality richterite and pargasite, also from Afghanistan. Fitted FTIR spectra in the OH-stretching region of the present samples accordingly corresponded to the spectrum of pargasite, with the strongest band at 3713 cm^{-1} (Figure 11). This excluded richterite (strongest band at 3730 cm^{-1}) as a possibility. However, Raman spectra seemed to more closely match the spectra of edenite in the RRUFF database, which show a principal band at 674 cm^{-1}, slightly shifted from the typical position for pargasite at 668 cm^{-1} (Figure 12).

Therefore, to confirm the identification of these samples, they were analysed by electron microprobe by authors MD and FCH. Based on three spot analyses on each stone, the analyses gave the following average compositions for the 0.27 ct (1) and 0.65 ct (2) specimens:

(1) $(Na_{0.87}K_{0.13})_{1.00}(Ca_{1.60}Na_{0.40})_2(Mg_{4.03}Al_{0.70}Ti_{0.09}Fe^{2+}_{0.02}Mn_{0.01})_{4.85}(Si_{6.82}Al_{1.18})_8O_{22}(OH_{1.67}F_{0.33})_2$

(2) $(Na_{0.85}K_{0.12})_{0.97}(Ca_{1.60}Na_{0.40})_2(Mg_{4.20}Al_{0.61}Ti_{0.09}Fe^{2+}_{0.02}Mn_{0.01})_{4.93}(Si_{6.79}Al_{1.21})_8O_{22}(OH_{1.69}F_{0.31})_2$

Considering the general formula $AB_2C_5T_8O_{22}W_2$ for amphibole supergroup minerals and their current classification (Hawthorne *et al.* 2012), the specimens clearly are calcium amphiboles, based on $^{B}Ca/^{B}(Ca+Na) = 0.8$. According to the compositional boundaries of calcium amphiboles, they plot nicely in the pargasite field, with $^{A}(Na+K+2Ca) = 1.00$ and 0.88, and $^{C}(Al+Fe^{3+}+2Ti) = 0.97$ and 0.79, respectively (Figure 13).

The current classification of amphiboles is based on the A, B and C cations, rather than on the A, B and T cations as proposed earlier by Leake *et al.* (1997). The 6.8 Si atoms at the T site would have classified these samples as edenite in this previous classification (5.5–6.5 Si for pargasite, >6.5 Si for edenite). This could explain the discrepancy of the Raman spectra indicating edenite, showing a main band at 674 cm^{-1}, which is assigned to vibration of bridging oxygen atoms (O_b) that link adjacent SiO_4 tetrahedra (Si–O_b–Si symmetrical stretching; Apopei & Buzgar 2010).

These examples show that there are limitations in the use of standard gemmological equipment and Raman spectroscopy to correctly identify an amphibole, and that reference Raman spectra of amphiboles need re-evaluation, updating (including the OH-stretching region in the higher spectral range) and further study.

Dr J. C. (Hanco) Zwaan FGA
(hanco.zwaan@naturalis.nl)
Netherlands Gemmological Laboratory
Naturalis Biodiversity Center
Leiden, The Netherlands

Maxwell C. Day and Dr Frank C. Hawthorne
University of Manitoba
Winnipeg, Manitoba, Canada

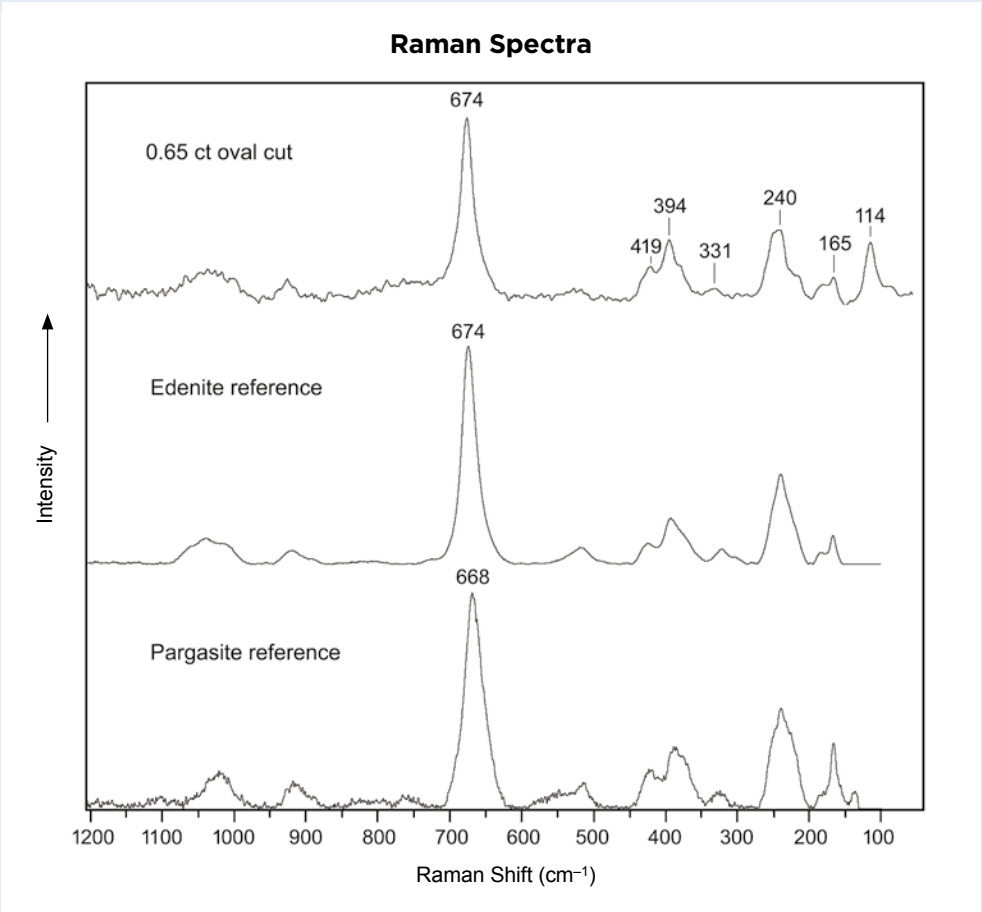

Figure 12: Raman spectra of both stones gave a best match with edenite spectra in the RRUFF database. The spectrum shown here is for the 0.65 ct sample.

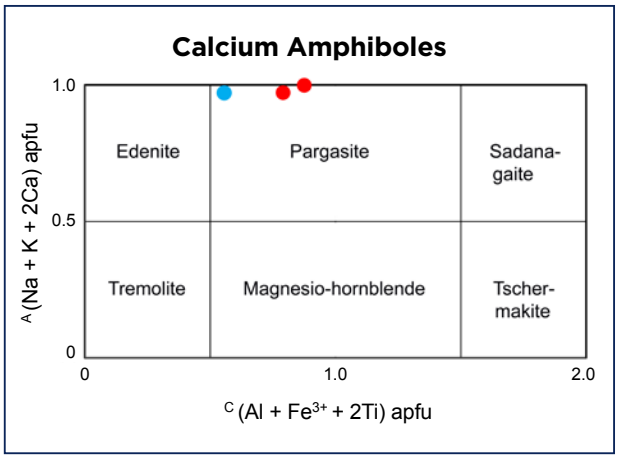

Figure 13: Compositional boundaries of calcium amphiboles show that the two faceted samples examined here (red dots) fall within the pargasite field. For comparison, the blue dot indicates the composition of a pargasite from Afghanistan analysed previously by Day *et al.* (2018).

References

Apopei, A.I. & Buzgar, N. 2010. The Raman study of amphiboles. *Analele Ştiinţifice ale Universităţii "Al. I. Cuza" Iaşi*, **56**(1), 57–83.

Day, M.C., Hawthorne, F.C., Susta, U., Della Ventura, G. & Harlow, G.E. 2018. Short-range order-disorder in gem richterite and pargasite from Afghanistan: Crystal-structure refinement and infrared spectroscopy. *Canadian Mineralogist*, **56**(6), 939–950, https://doi.org/10.3749/canmin.1800052.

Dedeyne, R. & Quintens, I. 2007. *Tables of Gemstone Identification*. Glirico, Gent, Belgium, 309 pp.

Hawthorne, F.C., Oberti, R., Harlow, G.E., Maresch, W.V., Martin, R.F., Schumacher, J.C. & Welch, M.D. 2012. Nomenclature of the amphibole supergroup. *American Mineralogist*, **97**(11–12), 2031–2048, https://doi.org/10.2138/am.2012.4276.

Leake, B.E., Woolley, A.R., Arps, C.E.S., Birch, W.D., Gilbert, M.C., Grice, J.D., Hawthorne, F.C., Kato, A. *et al.* 1997. Nomenclature of amphiboles: Report of the Subcommittee on Amphiboles of the International Mineralogical Association Commission on New Minerals and Mineral Names. *European Journal of Mineralogy*, **9**(3), 623–651, https://doi.org/10.1127/ejm/9/3/0623.